Articles

Synthesis and Optoelectronic Properties of Starlike Polyfluorenes with a Silsesquioxane Core

Wei-Jung Lin,[†] Wen-Chang Chen,*[,†,‡] Wen-Chung Wu,[†,§] Yu-Hua Niu,[§] and Alex K.-Y. Jen[§]

Department of Chemical Engineering and Institute of Polymer Science and Engineering, National Taiwan University, Taipei, Taiwan 10617 and Department of Materials Science and Engineering, Box 352120, University of Washington, Seattle, Washington 98195

Received January 5, 2004; Revised Manuscript Received February 12, 2004

ABSTRACT: A novel starlike polyfluorene derivative, **PFO-SQ**, was synthesized by the Ni(0)-catalyzed reaction of octa(2-(4-bromophenyl)ethyl)octasilsesquioxane (**OBPE-SQ**) and polydioctylfluoroene (**PFO**). The incorporation of the silsesquioxane core into polyfluorene could significantly reduce the aggregation as well as enhance the thermal stability. The DSC study showed an elimination of the glass transition and crystallization as well as a significant reduction of the melting enthalpy in **PFO-SQ**. The UV−vis absorption spectra in a different solvent combination or solid-state film showed an intensity reduction of the aggregation peak for **PFO-SQ** in comparison with that of **PFO**. The stability of the photoluminescence spectra of **PFO-SQ** could be up to 150 °C, while that of **PFO** showed a significant green emission at 530 nm. A single-layer LED device using **PFO-SQ** showed a turn on voltage of 6.0 V, a brightness of 5430 cd/m^2 (at a drive voltage of 8.8 V), and a current density of 0.844 A/cm^2. The maximum luminescence intensity and quantum efficiency of **PFO-SQ** were almost twice as good as those of the **PFO** electroluminescent device. Hence, the incorporation of the inorganic silsesquioxane core into polyfluorenes could provide a new methodology for preparing organic light-emitting diodes with improved thermal and optoelectronic characteristics.

Introduction

Conjugated polymers have been extensively studied for their potential applications in electroluminescent displays,[1] solar cells,[2] and thin film transistors.[3] Among many promising conjugated polymers, polyfluorenes (**PFO**) have been recognized as a candidate for blue light-emitting diodes (LED) because of their processibility, high fluorescence quantum yield, and good charge transport properties.[4−11] However, polyfluorenes tend to form aggregates and/or interchain excimers during device fabrication and operation, leading to a red-shifted emission and lower efficiency.[5−11] Recently, the red-shifted emission was also attributed to the emissive keto defect sites due to thermo- or electro-oxidative degradation of the polyfluorene backbone.[12] As a result, the pure blue emission was changed to an undesired blue-green color.

Various strategies have been used to reduce the formation of aggregation or keto defects in polyfluorenes, including (a) the introduction of bulky side chains or dendronization,[6c−g,9] (b) using spiro-linked[6b,7,8] or cross-linked[5b,10] structure, (c) copolymerization to induce disorder,[5a,6a,8] (d) improving oxidative stability of pendant groups[6h] or chain ends,[5c,9] and (e) blending with a high glass transition temperature polymer to limit the chain mobility.[11]

Organic−inorganic hybrid materials could improve the thermal stability of conjugated polymers as well as tune their morphology. The brightness and quantum efficiency of polyfluorenes was improved by incorporating a bulky polyhedral oligomeric silsesquioxane (POSS) into the chain end.[9] The significantly enhanced electroluminescent characteristics were attributed to the reduction of aggregation/excimers or lower keto defects. However, the reported monosubstituted POSS had only one reactive functional site and thus used as end-capping group for the **PFO**, which might limit the enhancement of thermal stability or possibly the degree of decreasing excimer formation. Therefore, developing new polymer architecture based on the POSS could be of both scientific and application interest.

In this study, starlike polyfluorene based on a silsesquioxane core was synthesized and characterized, as shown in Schemes 1 and 2. A new silsesquioxane core, octa(2-(4-bromophenyl)ethyl)octasilsesquioxane **(OBPE-SQ)**, was synthesized by the hydrosilylation reaction of 4-bromostyrene with octa(hydrido)octasilsesquioxane (**T_8**). The **OBPE-SQ** then served as a core to couple with the dibromo chain end of poly(dioctylfluorene) by Ni(0)-catalyzed coupling. The starlike **PFO-SQ** could not only be used as a bulky group to reduce the aggregation of the **PFO** but also enhance the thermal stability by

* To whom correspondence should be addressed. Phone: 886-2-23628398. Fax: 886-2-23623040. E-mail: chenwc@ntu.edu.tw.
† Department of Chemical Engineering, National Taiwan University.
‡ Institute of Polymer Science and Engineering, National Taiwan University.
§ University of Washington.

10.1021/ma0499573 CCC: $27.50
Published on Web 03/12/2004

Scheme 1. Synthesis of T_8 and OBPE-SQ

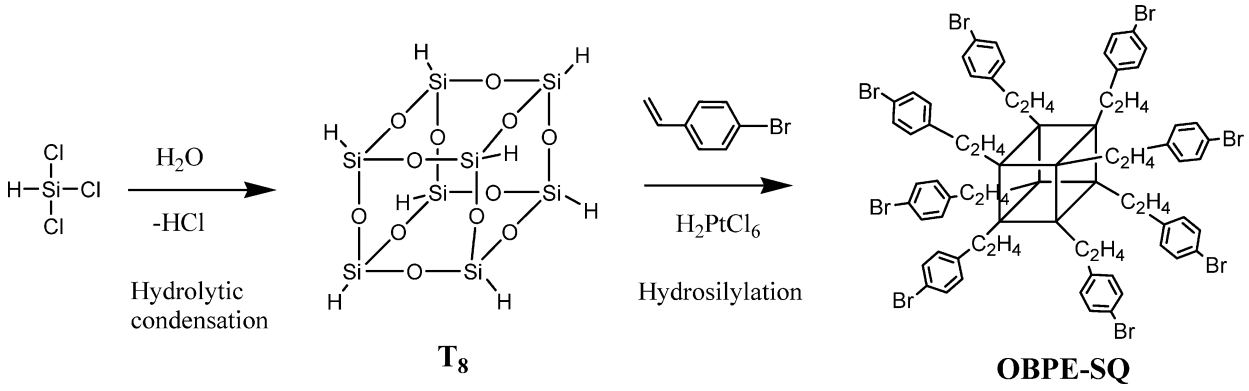

Scheme 2. Synthesis of PFO and PFO-SQ

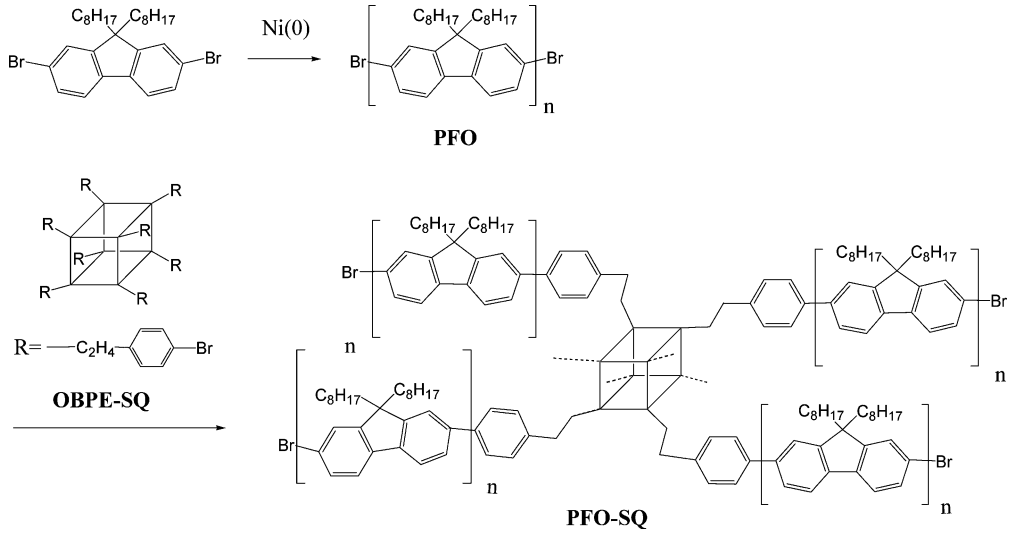

the inorganic core. The chemical structure, thermal properties, and optoelectronic characteristics are reported in the present study.

Experimental Section

Materials. Trichlorosilane ($HSiCl_3$, 98%, Acros), 4-bromostyrene (98%, Acros), 9,9-dioctyl-2,7-dibromofluorene (96%, Aldrich), hydrogen hexachloroplatinate(IV) (H_2PtCl_6, 99%, Acros), bis(1,5-cyclooctadiene)nickel(0) (99%, Aldrich), 2,2′-dipyridyl (99+%, Aldrich), 1,5-cyclooctadiene (99+%, Aldrich), ultra-anhydrous-grade toluene (99.9%, TEDIA), and dimethylformamide (DMF, 99.9%, TEDIA) were used without further purification.

*Synthesis of Octa(2-(4-bromophenyl)ethyl)octasilsesquioxane (**OBPE-SQ**).* Octa(hydrido)octasilsesquioxane (**T_8**) was synthesized by the hydrolytic condensation reaction of trichlorosilane.[13] Then, **OBPE-SQ** was prepared by the hydrosilylation reaction of 4-bromostyrene with (**T_8**), as shown Scheme 1. The details of the synthesis follow. H_2PtCl_6 was dissolved in 2-methoxyethyl to form a 1 wt % solution before use. In a 50 mL flask, **T_8** (1.24 g, 2.93 mmol) was dissolved in 4-bromostyrene (12.84 g, 70.2 mmol). Three drops of H_2PtCl_6 solution was then added. In the following, the solution was refluxed at 115 °C for 6 h under nitrogen atmosphere. After cooling the reaction mixture to ambient temperature, the product was precipitated into stirring methanol, filtered, dissolved in acetone, and then precipitated in methanol again. The above purification procedures were repeated twice. The obtained product was then dried in a vacuum at 60 °C for 12 h. A colorless, highly viscous, and fluidlike product with the yield of 67% (3.7 g) was thus obtained. ^{1}H NMR (500 MHz, $CDCl_3$, ppm): 7.1−7.5 (m, 32H, aromatic CH), 2.65 (br, 13.4H, CH_2–CH_2–Ar, β adduct), 2.25 (br, 1.3H, −CH(CH_3)−Ar, α adduct), 1.4 (br, 3.9H, −CH(CH_3)−Ar, α adduct), 0.9 (br, 13.4H, −Si−CH_2–CH_2, β adduct). ^{13}C NMR (100 MHz, $CDCl_3$, ppm): δ 142.4, 131.3, 129.6, 119.5, 28.2, 13.3. ^{29}Si NMR (100 MHz, $CDCl_3$, ppm): −66.5. Anal. Calcd for $C_{64}H_{64}Br_8O_{12}Si_8$ (%): C, 40.68; H, 3.39. Found (%): C, 40.42; H, 3.36.

Synthesis of Poly(9,9-dioctylfluorene) (PFO). The synthesis of **PFO** used a similar procedure to that reported in the literature.[5] Anal. Calcd for $C_{29}H_{40}$ (%): C, 89.69; H, 10.31. Found: C, 89.00; H, 10.44.

Synthesis of Starlike Polyfluorene Using the Silsesquioxane as the Core (**PFO-SQ**). A 170 mg (0.64 mmol) amount of bis-(1,5-cyclooctadiene)nickel(0), 100 mg (0.64 mmol) of 2,2′-bipyridyl, and 69.2 mg (0.64 mmol) of 1,5-cyclooctadiene were added to a 50-mL flask containing 10 mL of DMF and 10 mL of toluene. The solution was preheated at 60 °C under nitrogen atmosphere for 30 min. Then, 190 mg of **PFO** (0.014 mmol based on the number-average molecular weight (M_n) of 14 000) and 10 mg of **OBPE-SQ** (0.0053 mmol) were added into the flask. The mixture was heated at 100 °C for 6 h and then poured into 200 mL of stirring methanol. The precipitate was washed with hydrochloric acid and acetone. Then, 189 mg of crude product was obtained (91.7% yield). The crude product was dissolved into chloroform, and the insoluble fraction was filtered out and dried in a vacuum at 60 °C for 12 h. A 140 mg amount of the chloroform-soluble part and 40 mg of the chloroform-insoluble part were obtained. Characterization of the chloroform-soluble fraction is given below. IR (KBr, cm^{-1}): 2930 and 2850 (alkyl C−H), 1460 (ring), 1120 (Si−O−Si), and 810 (aryl C−H, wag). ^{1}H NMR (500 MHz, ppm, $CDCl_3$): δ 7.8 (br, 2H), 7.6 (br, 4H), aliphatic δ 2.12 (br, 4H), 1.14 (br, 20H), 0.80 (m, 10H). Anal. found for **PFO-SQ**. (1) Soluble part in chloroform (77.8%): C, 87.82; H, 10.11. (2) Insoluble part in chloroform (22.2%): C, 82.25; H, 9.34.

Characterization. ^{1}H, ^{13}C, and ^{29}Si nuclear magnetic resonance (NMR) data were obtained by a Bruker AV 500 MHz spectrometer. Fourier transform infrared (FTIR) spectra of the synthesized materials were obtained by a Digilab FTS 3500GX with a resolution of 4 cm^{-1}. Gel permeation chromatographic analysis was performed on a Lab Alliance RI2000 instrument (two columns, MIXED-C and D from Polymer Laboratories) connected with one refractive index detector from Schambeck SFD Gmbh. All GPC analyses were performed on polymer/THF solution at a flow rate of 1 mL/min at 40 °C and calibrated with polystyrene standards.

Thermogravimetric analysis (TGA) and differential scanning calorimetry (DSC) measurements were performed under a nitrogen atmosphere at a heating rate of 20 and 10 °C/min using a TA instrument TGA-951 and DSC-910S, respectively. UV−vis absorption and photoluminescence (PL) spectra were recorded on a Jasco model UV/VIS/NIR V-570 spectrophotometer and FP-6200 spectrofluorometer, respectively. For the solution spectra, polymers were dissolved in chloroform ($\sim 10^{-6}$ M) and then put in a quartz cell for measurement. For the thin film spectra, polymers were first dissolved in chloroform (1 wt %) and then spin-coated on glass substrates at 1000 rpm for 30 s. Then, the film samples were dried at 50 °C under vacuum. The solution PL quantum efficiencies (Φ_{PL}) were measured by excitation of the respective polymer solutions at 380 nm and compared with the solution emission of quinine sulfate in 0.5 M H_2SO_4 (ca. 10^{-6} M solution, $\Phi_{PL} = 0.546$).[14] The solid-state Φ_{PL} was determined by comparing the PL of the respective polymer films ($\lambda_{ex} = 380$ nm) with the PL of the fresh **PFO** film ($\Phi_{PL} = 0.55$).[4c,10b] For investigating the thermal stability of the prepared polymers, films were annealed on a hot plate in air at 100, 150, and 200 °C for 1 h, each. For investigating the keto defects from FTIR, films were annealed at 200, 225, and 250 °C for 1 h each, respectively.

Device Fabrication and Testing. The electroluminescent (EL) devices were fabricated on an ITO-coated glass substrate that was precleaned and oxygen plasma treated before use. A layer of poly(ethylene dioxythiophene):poly(styrene sulfonate) (PEDOT:PSS, Baytron P from Bayer Co.), 40 nm thick, was formed by spin-coating from its aqueous solution (1.3 wt %). The EL layer was spin-coated at 2000 rpm from the corresponding *p*-xylene solution (15 mg mL^{-1}) on top of the vacuum-dried PEDOT:PSS layer. The nominal thickness of the EL layer was 65 nm. Under a base pressure below 1×10^{-6} Torr, a layer of Ca (30 nm) was vacuum deposited as cathode and a thick layer of Ag was deposited subsequently as the protecting layer.

Current−voltage characteristics were measured with a Hewlett-Packard 4155B semiconductor parameter analyzer. The power of EL emission was measured using a Newport 2835-C multi-function optical meter. The brightness was calculated using the forward output power and the EL spectra of the devices, assuming Lambertian distribution of the EL emission.

Results and Discussion

Synthesis of the OBPE-SQ. Figure 1 shows the FTIR spectra of **T_8**, **OBPE-SQ**, **PFO**, and **PFO-SQ**. The spectrum of **T_8** shows three major characteristic peaks at 2250 (Si−H stretching), 1120 (Si−O−Si stretching), and 860 cm^{-1} (Si−H bending). The Si−H stretching band at 2250 cm^{-1} completely disappears in the FTIR spectrum of **OBPE-SQ**. The ^{1}H NMR spectrum also showed that the Si−*H* bond ($\delta = 4.23$ ppm) of **T_8** is not present in that of **OBPE-SQ**. The Si−C band (at 1074 cm^{-1}) overlaps with the Si−O−Si band and thus could not be clearly observed in the FTIR spectrum. However, formation of the Si−C bond at δ 13.3 ppm was observed in the ^{13}C NMR spectrum of **OBPE-SQ**. Moreover, the ^{29}Si NMR spectra of **T_8** and **OBPE-SQ** showed a single Si−H(cage) peak and a Si−C(alkyl, cage) peak at −84.5 and −66.5 ppm, respectively, providing further evidence for intact cage structure.[15] The formation of α- and *β*-adducts of **OBPE-SQ** was observed in both the ^{1}H and ^{13}C NMR spectra (see Supporting Information). The proportion of the *β*-adduct (84%) of **OBPE-SQ** was higher than that of the α-adduct (16%) due to steric hindrance, which was similar to other silsesquioxane derivatives reported in the literature.[15a] The FTIR band at 1456 cm^{-1} in the **OBPE-SQ** spectrum is assigned to the phenyl ring stretching. Both the NMR and FTIR results suggested that **T_8** was functionalized by bromophenylethyl through the hydrosilylation reaction. It is important for **T_8** to be fully functionalized because any remaining Si−H would be thermally unstable and chemically reactive to base and water. The synthesized **OBPE-SQ** with eight reactive functional sites could be further reacted with conjugated polymers by Suzuki coupling, Heck reaction, or Yamamoto coupling.

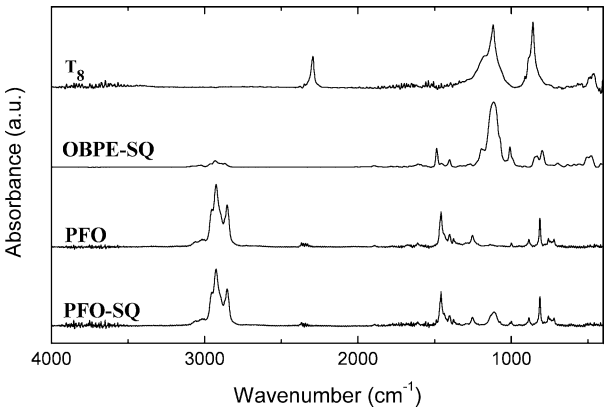

Figure 1. FTIR spectra of **T_8**, **OBPE-SQ**, **PFO**, and **PFO-SQ**.

The carbon and hydrogen contents of **OBPE-SQ** from the elemental analysis are in a good agreement with the theoretical values. The arm number of **OBPE-SQ** is estimated to be 7.9 based on the C content from elemental analysis. The number-average molecular weight (M_n) and PDI of **OBPE-SQ** estimated from GPC are 1196 and 1.02, respectively. The M_n is lower than the theoretical molecular weight of 1888. The underestimated value could be explained by its spherical structure compared to the linear structure of the polystyrene standard.[16] However, the narrow PDI, the consistent elemental analysis, and the NMR and FTIR results described in the previous paragraph suggest the successful synthesis of **OBPE-SQ**.

Synthesis of PFO-SQ. The FTIR spectra of **PFO** and **PFO-SQ** are also shown in Figure 1. The absorption bands in the IR spectrum of **PFO** are similar to those reported in the literature.[10a] The Si−O−Si absorption band at 1120 cm^{-1} shown in the spectrum of **PFO-SQ** indicates the successful incorporation of the silsesquioxane core into **PFO**, since it is not shown in that of **PFO**. The similar Si−O−Si peak position of **PFO-SQ** with those of **T_8** and **OBPE-SQ** also suggests retention of the cage structure in the synthesized polymer. Note that the Si−O−Si peak position of the silsesquioxane cage would be shifted to a lower wavenumber at 1120 cm^{-1} if it was structurally transformed to an unsymmetrical structure.[17] The ^{1}H and ^{13}C NMR of **PFO** and **PFO-SQ** were almost identical because of the low POSS content around 3.8 wt % in **PFO-SQ**.

The molecular weights (M_w, M_n) of **PFO** and **PFO-SQ** estimated from GPC were 33 000, 14 000 and 65 000, 17 000, respectively. The higher molecular

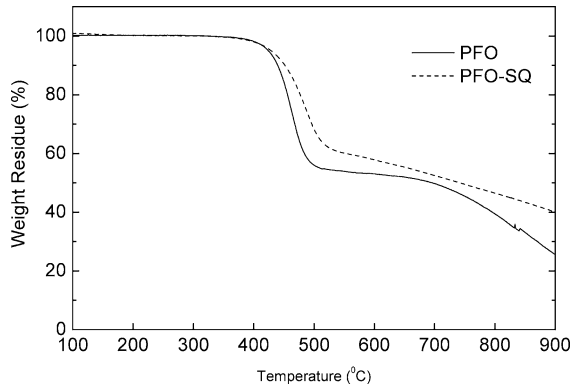

Figure 2. TGA curves of **PFO** and **PFO-SQ** at a heating rate of 20 °C/min under nitrogen atmosphere.

weight of the latter suggests attachment of the **PFO** as the arm of the silsesquioxane core. For an eight-arm starlike **PFO-SQ**, the weight percent of **OBPE-SQ** is 1.7% by using the M_n of 14 000 and 1888, respectively. However, the weight percent of **OBPE-SQ** in **PFO-SQ** estimated from elemental analysis is 3.8 wt %, which corresponds to an average number of 3.5. On the other hand, the molecular weights of conjugated polymers are generally overestimated because of their rodlike conformation. For example, the molecular weight of poly(3-hexylthiophene) estimated GPC was 75 000, but that from MALDI-TOF MS spectra was 36 000.[18] Hence, the average arm number could be 7 if the estimated M_n of the **PFO** was 7000. Nevertheless, both GPC and elemental analysis results suggest **PFO-SQ** is a starlike polymer consisting of **PFO** arms on the silsesquioxane core.

The weight percent of **OPBE-SQ** in **PFO-SQ** is lower than the original feed ratio of 5%. It is due to the removal of the cross-linked **PFO** resulting from the bromide coupling reaction on the two ends of **PFO**. For the current interest of the soluble conjugated polymers on device applications, only the properties and device characteristics of the chloroform-soluble **PFO-SQ** were investigated.

Thermal Properties. Figure 2 shows the TGA curves of **PFO** and **PFO-SQ**, which show the thermal decomposition temperatures (T_d, 95 wt % residue) at 424 and 429 °C, respectively. The order of T_d and the 900 °C residue are on the same order of **PFO-SQ** > **PFO**, which suggests that the incorporation of the silsesquioxane core could enhance the thermal stability of **PFO**. Figure 3 shows the DSC curves for the **PFO** and **PFO-SQ**. The DSC curve of **PFO** shows three major transitions: a glass transition (T_g) at 63 °C, a crystallization exothermal peak at 93 °C, and a melting endothermal peak at 154 °C.[4a] However, only a small melting peak at 158 °C appears for **PFO-SQ**. It has been reported that the spiro-linked[7a] or cross-linked[5b] structure could raise or even eliminate T_g. The insignificant T_g in **PFO-SQ** suggests that the polymer chain mobility is largely suppressed by the silsesquioxane core. Also, the absence of a crystallization peak indicates that the silsesquioxane prevents the polymer chain from packing regularity. It might be attributed to the 3-D linkage of silsesquioxane with the **PFO** extending in a different direction since conjugated polymers are rigid and difficult to bend. The enthalpy of the melting peak for **PFO-SQ** was 5.7 J/g, which was smaller than that of **PFO** with 9.0 J/g. The DSC results suggested that **PFO-SQ** significantly reduced the chain mobility and packing ability of **PFO**.

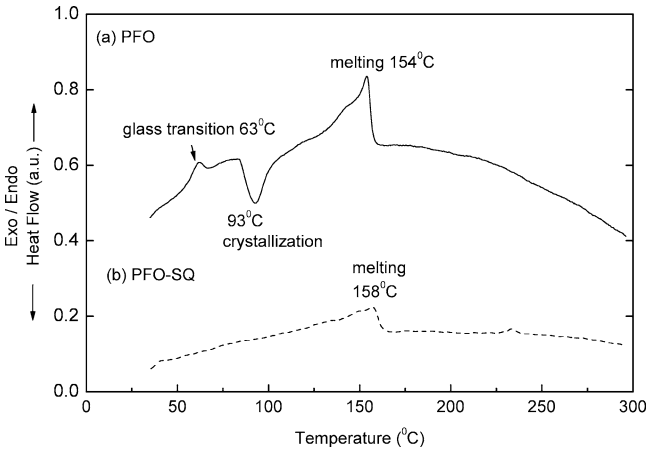

Figure 3. DSC curves of (a) **PFO** and (b) **PFO-SQ** at a heating rate of 10 °C/min under nitrogen atmosphere.

Optoelectronic Properties

Absorption and Photoluminescence. The solution of **PFO** and **PFO-SQ** in chloroform shows almost identical absorption and emission peaks (see Supporting Information). The peak maxima (λ_{max}) of the absorption and emission are 384 and 417 nm, respectively, which are similar to those reported in the literature.[4] However, a slight difference is observed on the spectrum shoulder at >500 nm, which is due to the aggregation/excimer formation. Since chloroform is a good solvent for **PFO**, almost no aggregation band is shown in the spectra. However, a new absorption peak at 437 nm due to aggregation appears if the polymer is dissolved in a poor solvent (equal volume mixture of chloroform and dichloroethane). The absorption intensity of the aggregation peak at 437 nm is smaller in **PFO-SQ** than **PFO**. Also, the λ_{max} of the emission spectrum of the **PFO** shows a 6 nm shift from 416 nm in chloroform to 422 nm in the mixed solvent but only a 3 nm shift for the case of **PFO-SQ**. Moreover, the aggregation/excimer formation at >500 nm is smaller in **PFO-SQ** than **PFO**. The solution quantum efficiency of **PFO-SQ** is 0.74, which is slightly higher than that of **PFO** with 0.72.

Figure 4a shows the normalized absorption and photoluminescent spectra of **PFO** and **PFO-SQ** films. Similar conclusions on λ_{max} and the intensity of the peak shoulder are obtained in the comparison of **PFO** and **PFO-SQ** as those discussed in the solution spectra. **PFO-SQ** also shows a higher PL quantum efficiency of 0.64 than that of **PFO** with 0.55. These results suggest that incorporation of the silsesquioxane core into the **PFO** could suppress the formation of aggregates. However, the difference on the aggregation absorption band around 435 nm was not observed between **PFO** and **PFO** end-capped POSS in the literature.[9] It might be due to the difference of the molecular architecture (starlike in the present study and end-capped in the literature[9]) or the silsesquioxane content. Note that the silsesquioxane content in **PFO-SQ** and POSS end-capped **PFO**[9] are 3.8% and 1.2%, respectively.

Color and luminescence stability under elevated temperatures are very important polymer LED since the temperature inside the devices could exceed 86 °C depending on the operating conditions.[19] The significance of incorporation of the silsesquioxane core into **PFO** on the luminescence properties is shown by heating the films. Parts b, c, and d of Figure 4 show the normalized absorption and PL emission spectra of the annealed

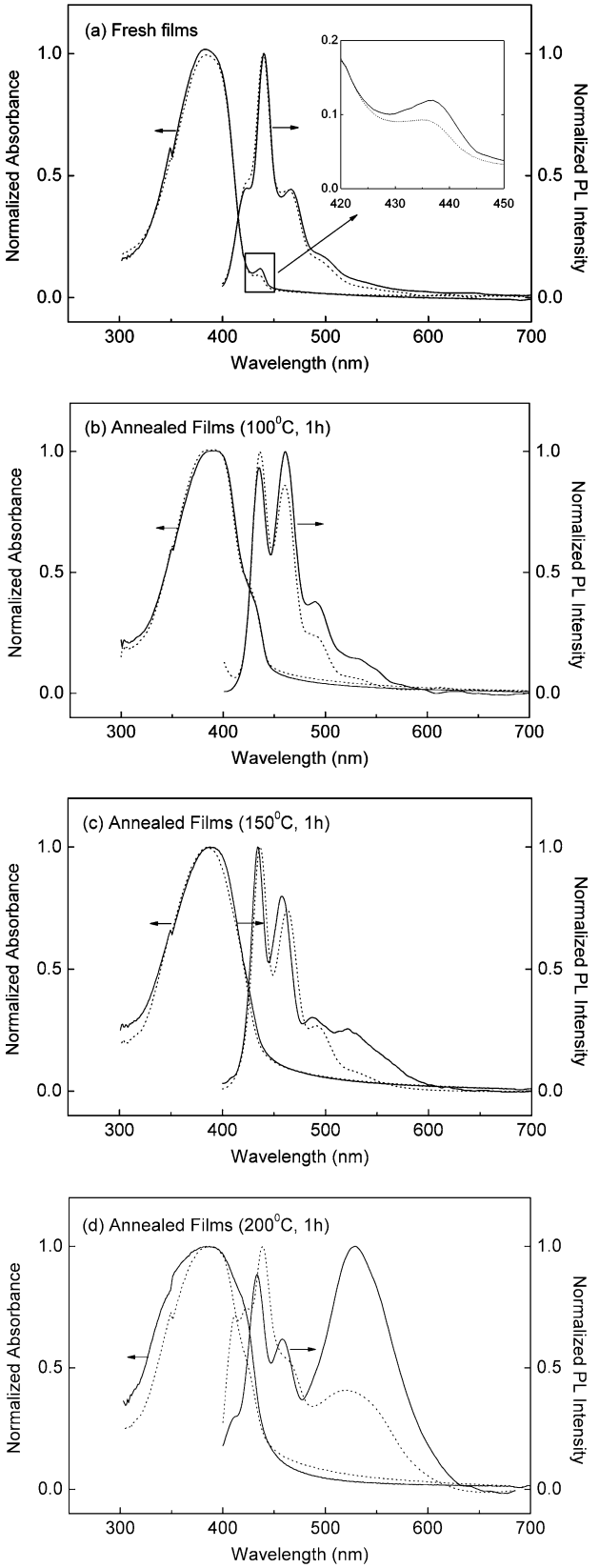

Figure 4. Normalized UV−vis absorption and photoluminescence (PL) spectra of **PFO** (solid line) and **PFO-SQ** (dotted line) spin-coated films after the following treatment: (a) fresh films, annealed at (b) 100, (c) 150, and (d) 200 °C for 1 h each.

PFO and **PFO-SQ** films at 100, 150, and 200 °C for 1 h each, respectively. In Figure 4b, the **PFO** film annealed at 100 °C shows an additional emission at a longer wavelength of 490 nm in comparison with the fresh films while the absorption λ_{max} remained at 385 nm. However, the PL spectrum of **PFO-SQ** only shows a small shoulder under similar heating conditions. The unchanged absorption λ_{max} before and after heating suggests that the polymer did not change its conjugation after thermal treatment. By further increasing the heating temperature to 150 °C (Figure 4c), the green emission peak at 530 nm appeared in **PFO** but only an insignificant shoulder above 500 nm for **PFO-SQ**. As shown in Figure 4d, a strong green emission near 530 nm is shown in the spectrum of **PFO** but that of **PFO-SQ** shows a lower intensity after annealing at 200 °C for 1 h. Since the heating temperature of 200 °C was higher than the melting temperatures of both **PFO** and **PFO-SQ**, the 530 nm peak shown in Figure 4d might be mostly due to the keto defect. The PL spectral stability of **PFO-SQ** at 150 °C is similar to other polyfluorene deivatives reported in the literature.[5b,7,10] Besides, the quantum yield of **PFO-SQ**-annealed film is higher than that of **PFO** for the case of Figure 4b−d. These results suggest that the starlike **POF-SQ** could reduce either the aggregation or the keto defect in comparison with **PFO**.

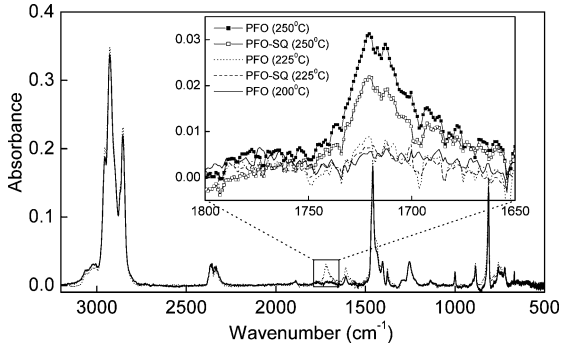

Figure 5. FTIR spectra of **PFO** and **PFO-SQ** films after baking at 200 or 250 °C for 1 h. The inset shows the magnified >C═O stretching mode at 1721 cm^{-1}.

The origin of the green emission in polyfluorene-based conjugated polymer has been mostly attributed to aggregate/excimer formation or keto defects.[5−12] Direct evidence of a keto defect was that **PFO** showed a keto (C═O) characteristic IR peak at 1721 cm^{-1} after being photooxidized for several minutes.[12a] If the curing temperature is heated above the melting temperature, the defect would be mostly due to the keto defect. Figure 5 shows the FTIR spectra of **PFO** and **PFO-SQ** after baking at various temperatures for 1 h each. Below 200 °C, no obvious keto peak was found for both polymers. The keto peak appears initially at 225 °C, and the intensity grows stronger at 250 °C, as shown in Figure 5. The normalized intensity of the keto peak on **POF-SQ** is smaller than that of **PFO**. As a result, **PFO-SQ** could also suppress part of the keto formation by enhancing the thermal-oxidative stability besides the aggregation.

Electroluminescence (EL) Characteristics. Figure 6 shows the electroluminescence (EL) spectra of **PFO** and **PFO-SQ** devices. Both EL devices show a green emission around 530 nm due to the aggregation/excimers formation or the keto defects as discussed previously. The intensity of the green emission on the **PFO** EL device is higher than those reported in the literature.[4,9,10] It might be due to the molecular weight of the **PFO** used in the present study being smaller than those reported in the literature.[4,9,10] Hosoi et al. reported

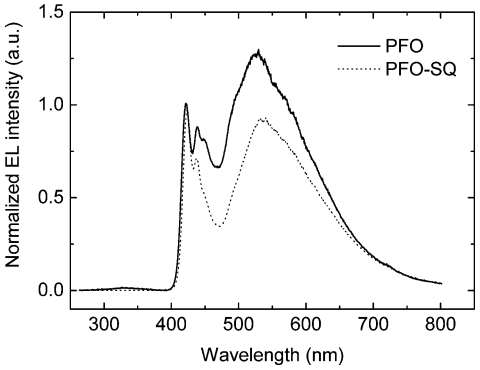

Figure 6. Electroluminescent (EL) spectra of the LED devices based on **PFO** and **PFO-SQ** with the device configuration: ITO/PEDOT:PSS/polymers/Ca/Ag.

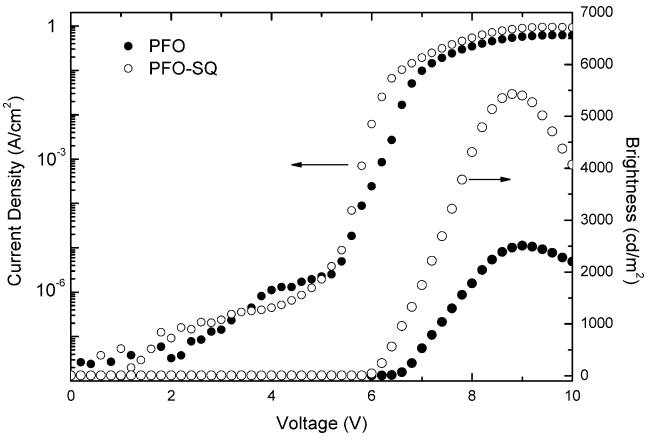

Figure 7. Variation of the current density and brightness with the driven voltage for the EL devices based on the **PFO** (●) and **PFO-SQ** (○).

that the EL characteristics of the high molecular weight **PFO** were superior to those of the low molecular weight **PFO**.[20] Weinfurtner et al. also found that low molecular weight polymer fraction was responsible for aggregation in the liquid crystalline **PFO**.[21] However, the green emission of **PFO-SQ** at 530 nm was lower than that of **PFO**, which is consistent with PL result. Figure 7 shows the variation of the current density and brightness of the EL devices based on **PFO** and **PFO-SQ**, respectively. The curves of current density versus voltage are similar in the two devices. This suggests that incorporation of silsesquioxane did not affect the charge transport ability of **PFO**. However, the turn-on voltage was decreased from 6.4 V for the **PFO** EL device to 6.0 V for **PFO-SQ**, which is similar to that of the silsesquioxane end-capped **PFO**.[9] Besides, the current density of the **PFO-SQ** EL device quickly turned on from 5.5 to 6 V and increased sharply from 10^{-6} to 10^{-1} A/cm^2. A significant enhancement of the brightness from the **PFO** EL device to **PFO-SQ** is also shown in Figure 7. The maximum brightness of the **PFO-SQ**-based device reaches 5430 cd/m^2 at a drive voltage of 8.8 V and a current density of 0.844 A/cm^2. However, the maximum brightness of the **PFO** EL device is 2510 cd/m^2 at the driving voltage of 9.0 V. This is an enhancement of the brightness that is almost twice that from the **PFO** EL device to that of **PFO-SQ**. The maximum external quantum efficiency of the **PFO-SQ** EL device is 0.42% at a brightness of 960 cd/m^2 with a driving voltage of 6.6 V but 0.24% at 788 cd/m^2 and 7.2 V for the case of **PFO**. The improved brightness and quantum efficiency in the case of the **PFO-SQ** EL device might be due to the reduction of the aggregates/excimers, the lower concentration of the keto defect, or the improved adhesion to ITO glass substrate for the incorporation of the silsesquioxane core.

Conclusions

We have successfully synthesized a novel starlike polyfluorene with silsesquioxane as the core. Incorporation of the silsesquioxane core into polyfluorene could significantly reduce aggregation as well as enhance the thermal stability. The DSC study showed elimination of the glass transition and crystallization as well as significant reduction on the melting enthalpy in **PFO-SQ**. The UV−vis absorption spectra in a different solvent combination or solid-state film show an intensity reduction of the aggregation peak for **PFO-SQ**. The stability of the photoluminescence spectra of **PFO-SQ** could be up to 150 °C, while that of **PFO** showed a significant green emission. A single-layer LED device using **PFO-SQ** showed a turn-on voltage of 6.0 V, a brightness of 5430 cd/m^2 (at a drive voltage of 8.8 V), and a current density of 0.844 A/cm^2. The maximum luminescence intensity and quantum efficiency of **PFO** were almost twice as good as those of the **PFO** EL device. Hence, incorporation of the inorganic silsesquioxane core into polyfluorenes could provide a new methodology for preparing organic light-emitting diodes with improved thermal and optoelectronic characteristics.

Acknowledgment. We thank the financial support from the National Science Council, the Ministry of Economic Affairs, and the Department of Education of Taiwan. The helpful discussion with Professor Chain-Shu Hsu of National Chiao-Tung University of Taiwan is also highly appreciated.

Supporting Information Available: ^{1}H NMR, ^{13}C NMR, and ^{29}Si NMR spectra of **OBPE-SQ**. ^{1}H NMR and ^{13}C NMR spectra of **PFO-SQ**. Absorption spectra of normalized UV−vis absorption and photoluminescence spectra of **PFO** and **PFO-SQ** dissolved in (a) good solvent (chloroform) and (b) poor solvent (chloroform/dichloroethane = 1:1). This material is available free of charge via the Internet at http://pubs.acs.org.

References and Notes

(1) (a) Burroughes, J. H.; Bradley, D. D. C.; Brown, A. R.; Marks, R. N.; Mackay, K.; Friend, R. H.; Burns, P. L.; Holmes, A. B. *Nature* **1990**, *347*, 539. (b) Gustafsson, G.; Cao, Y.; Treacy, G. M.; Klavetter, F.; Colaneri, N.; Heeger, A. J. *Nature* **1992**, *357*, 477. (c) Greenham, N. C.; Moratti, S. C.; Bradley, D. D. C.; Friend, R. H.; Holmes, A. B. *Nature* **1993**, *365*, 628. (d) Jenekhe, S. A.; Osaheni, J. A. *Science* **1994**, *620*, 765.

(2) (a) Halls, J. J. M.; Walsh, C. A.; Greenham, N. C.; Marseglia, E. A.; Friend, R. H.; Moratti, S. C.; Holmes, A. B. *Nature* **1995**, *376*, 498. (b) Yu, G.; Gao, J.; Hummelen, J. C.; Wudl, F.; Heeger, A. J. *Science* **1995**, *270*, 1789. (c) Granström, M.; Petritsch, K.; Arias, A. C.; Lux, A.; Andersson, M. R.; Friend, R. H. *Nature* **1998**, *395*, 257.

(3) (a) Yang, Y.; Heeger, A. J. *Nature* **1994**, *372*, 344. (b) Brown, A. R.; Pomp, A.; Hart, C. M.; de Leeuw, D. M. *Science* **1995**, *270*, 972. (c) Sirringhaus, H.; Tessler, N.; Friend, R. H. *Science* **1998**, *280*, 1741. (d) Sirringhaus, H.; Brown, P. J.; Friend, R. H.; Nielsen, M. M.; Bechgaard, K.; Langeveld-Voss, B. M. W.; Spiering, A. J. H.; Janssen, R. A. J.; Meijer, E. W.; Herwig, P.; de Leeuw, D. M. *Nature* **1999**, *401*, 685. (e) Babel, A.; Jenekhe, S. A. *J. Am. Chem. Soc.* **2003**, *125*, 13656.

(4) (a) Grell, M.; Bradley D. D. C.; Inbasekaran, M.; Woo, E. P. *Adv. Mater.* **1997**, *9*, 798. (b) Grell, M.; Bradley, D. D. C.; Long, X.; Chamberlain, T.; Inbasekaran, M.; Woo, E. P.; Soliman, M. *Acta Polym.* **1998**, *49*, 439. (c) Grice, A. W.; Bradley D. D. C.; Bernius, M. T.; Inbasekaran, M.; Wu, W. W.; Woo, E. P. *Appl. Phys. Lett.* **1998**, *73*, 629. (d) Friend, R. H.; Gymer, R. W.; Holmes, A. B.; Burroughes, J. H.; Marks,

R. N.; Taliani, C.; Bradley, D. D. C.; Dos Santos, D. A.; Bredas, J. L.; Logdlund, M.; Salaneck, W. R. *Nature* **1999**, *397*, 121. (e) Grell, M.; Bradley, D. D. C.; Ungar, G.; Hill, J.; Whitehead, K. S. *Macromolecules* **1999**, *32*, 5810.

(5) (a) Kreyenschmidt, M.; Klaerner, G.; Fuhrer, T.; Ashenhurst, J.; Karg, S.; Chen, W. D.; Lee, V. Y.; Scott, J. C.; Miller, R. D. *Macromolecules* **1998**, *31*, 1099. (b) Klarner, G.; Lee, J. I.; Lee, V. Y.; Chan, E.; Chen, J. P.; Nelson, A.; Markiewicz, D.; Siemens, R.; Scott, J. C.; Miller, R. D. *Chem. Mater.* **1999**, *11*, 1800. (c) Lee, J. I.; Klaerner, G.; Miller, R. D. *Chem. Mater.* **1999**, *11*, 1083.

(6) (a) Marsitzky, D.; Klapper, M.; Mullen, K. *Macromolecules* **1999**, *32*, 8685. (b) Marsitzky, D.; Murray, J.; Scott, J. C.; Carter, K. R. *Chem. Mater.* **2001**, *13*, 4285. (c) Marsitzky, D.; Vestberg, R.; Blainey, P.; Tang, B. T.; Hawker, C. J.; Carter, K. R. *J. Am. Chem. Soc.* **2001**, *123*, 6965. (d) Setayesh, S.; Grimsdale, A. C.; Weil, T.; Enkelmann, V.; Mullen, K.; Meghdadi, F.; List, E. J. W.; Leising, G. *J. Am. Chem. Soc.* **2001**, *123*, 946. (e) Ego, C.; Grimsdale, A. C.; Uckert, F.; Yu, G.; Srdanov, G.; Mullen, K. *Adv. Mater.* **2002**, *14*, 809. (f) Pogantsch, A.; Wenzl, F. P.; List, E. J. W.; Leising, G.; Grimsdale, A. C.; Mullen, K. *Adv. Mater.* **2002**, *14*, 1061. (g) Lupton, J. M.; Schouwink, P.; Keivanidis, P. E.; Grimsdale, A. C.; Mullen, K., *Adv. Funct. Mater.* **2003**, *13*, 154.

(7) (a) Wu, F. I.; Reddy, D. S.; Shu, C. F.; Liu, M. S.; Jen, A. K. Y. *Chem. Mater.* **2003**, *15*, 269. (b) Shu, C. F.; Dodda, R.; Wu, F. I.; Liu, M. S.; Jen, A. K. Y. *Macromolecules* **2003**, *36*, 6698.

(8) Zeng, G.; Yu, W. L.; Chua, S. J.; Huang, W. *Macromolecules* **2002**, *35*, 6907.

(9) Xiao, S.; Nguyen, M.; Gong, X.; Cao, Y.; Wu, H.; Moses, D.; Heeger, A. J. *Adv. Funct. Mater.* **2003**, *13*, 25.

(10) (a) Cho, H. J.; Jung B. J.; Cho, N. S.; Lee, J.; Shim, H. K. *Macromolecules* **2003**, *36*, 6704. (b) Lim, E.; Jung B. J.; Shim, H. K. *Macromolecules* **2003**, *36*, 4288.

(11) Kulkarni, A. P.; Jenekhe, S. A. *Macromolecules* **2003**, *36*, 5285.

(12) (a) List, E. J. W.; Guentner, R.; Freitas, P. S.; Scherf, U. *Adv. Mater.* **2002**, *14*, 374. (b) Omaner, L.; Pogantsch, A.; Freitas, P. S.; Scherf, U.; Gaal, M.; Zojer, E.; List, J. W. *Adv. Funct. Mater.* **2003**, *13*, 597. (c) Gaal, M.; List, E. J. W.; Scherf, U. *Macromolecules* **2003**, *36*, 4236. (d) Jacob, J.; Zhang, J.; Grimsdale, A. C.; Mullen, K.; Gaal, M.; List, J. W. *Macromolecules* **2003**, *36*, 8240.

(13) Agaskar, P. A. *Inorg. Chem.* **1991**, *30*, 2707.

(14) Eaton, D. F. *Pure Appl. Chem.* **1988**, *60*, 1107.

(15) (a) Crivello, J. V.; Malik, R. *J. Polym. Sci. Polym. Chem.* **1997**, *35*, 407. (b) Bolln, C.; Tsuchida, A.; Frey, H.; Mulhaupt, R. *Chem. Mater.* **1997**, *9*, 1475.

(16) (a)Choi, J.; Harcup, J.; Yee, A. F. *J. Am. Chem. Soc.* **2001**, *123*, 11420. (b) Tamaki, R.; Tanaka, Y.; Asuncion, M. Z.; Choi, J.; Laine, R. M. *J. Am. Chem. Soc.* **2001**, *123*, 12416. (c) Costa, R. O. R.; Vasconcelos, W. L.; Tamaki, R.; Laine, R. M. *Macromolecules* **2001**, *34*, 5398.

(17) (a) Liu, W. C.; Yang, C. C.; Chen, W. C.; Dai, B. T.; Tsai, M. S. *J. Non.-Cryst. Solids* **2002**, *311*, 233. (b) Chen, W. C.; Lee, L. H.; Chen, B. F.; Yen, C. T. *J. Mater. Chem.* **2002**, *12*, 3644. (c) Lee, L. H.; Chen, W. C.; Liu, W. C. *J. Polym. Sci. Polym. Chem.* **2002**, *40*, 1560. (d) Chen, W. C.; Lin, S.-C.; Dai, B.-T.; Tsai, M. S. *J. Electrochem. Soc.* **1999**, *146*, 3004. (e) Chen, W. C.; Yen, C.-T. *J. Vac. Sci. Technol.* B **2000**, *18*, 201.

(18) Liu, J.; Loewe, R. S.; McCullough, R. D. *Macromolecules* **1999**, *32*, 5777.

(19) Zhou, X.; He, J.; Liao, L. S.; Lu, M.; Ding, X. M.; Hou, X. Y.; Zhang, X. M.; He, X. Q.; Lee, S. T. *Adv. Mater.* **2000**, *12*, 265.

(20) Hosoi, K.; Mori, T.; Mizutani, T.; Yamamoto, T.; Kitamura, N. *Thin Solid Films* **2003**, *438*, 201.

(21) Weinfurtner, K. H.; Fujikawa, H.; Tokito, S.; Taga, Y. *Appl. Phys. Lett.* **2000**, *76*, 2502.

MA0499573